論　文（Original article）

Changes of above- and below-ground biomass forty-three years after a typhoon disturbance in a subalpine wave regeneration forest on Mt. Shimagare

Kojiro IWAMOTO[1)*], Shin UGAWA[2)], Masatake G. ARAKI[3)], Daisuke KABEYA[3)], Moriyoshi ISHIZUKA[4), 5)] and Takuya KAJIMOTO[3)]

Abstract

Understanding post-disturbance reforestation processes could make a valuable contribution towards predicting the impacts of future changes in disturbance regimes on forest ecosystems. In this study, we aimed to estimate biomass dynamics in a wave-regenerated fir forest following blowdown. Three research forest stands at different developmental stages (young, intermediate, and mature; 19, 36, and 59 years-old, respectively) were established in a wave-regenerated *Abies* forest on Mt. Shimagare in central Japan, where a severe large-scale windthrow event occurred during a typhoon landfall in 1959 (Typhoon "Vera"). For each stand, above- and below-ground biomass was estimated using tree census data measured repeatedly from 2001 to 2008 and size-mass allometric equations developed based on the sample trees' data. Growth patterns were also examined by tree ring analysis. The estimated biomass was the lowest in the young stand, but reached a similar level in both intermediate and mature stands. During the research period, mean height and estimated mass of trees were increasing in all sites but plot biomass were not increasing in the mature site because of mortalities of canopy trees. In the intermediate stand, tree ring analysis showed that post-typhoon seedlings could grow fast and thus a similar biomass accumulated to that in the mature stand, where trees originated from advanced seedlings that existed in high density prior to the disturbance. Compared to mature wave-regenerated fir forest without disturbance, mature forest in this study had lower biomass and the onset of mortality started earlier. These results suggest that typhoon disturbance affect subsequent forest structures and biomass accumulation.

Keywords: biomass dynamics, subalpine coniferous forest, wave-regeneration, typhoon disturbance

1. Introduction

Wave-regeneration is often observed in subalpine fir forests on slopes facing prevailing winds in several global regions, including Japan and northeastern North America (Iwaki and Totsuka 1959, Sprugel 1976, Boyce 1988, Kohyama 1988). Their landscapes are characterized by visible strips of dead trees between living stands, with a sequential arrangement between from smaller- to larger-sized trees down the slope. Wave-regeneration was long regarded as a shifting mosaic steady-state system, where waves of mortality (dead trees) move at a fairly uniform rate followed by continuous regeneration (Sprugel and Bormann 1981). Many studies have described the stand structure and dynamic features of wave-regenerated forests (e.g. Okubo 1933, Oshima et al. 1958, Sprugel 1976, Tadaki et al. 1977, Kohyama and Fujita 1981, Kimura 1982, Ugawa et al. 2007). Without catastrophic disturbance such as severe blowdown, strips of new dead trees were observed year by year at the edges of mature stands in the windward direction. Several causes of tree mortality at the forest edge have been postulated: needle death by rime ice deposition (Marchand et al. 1986, Boyce 1988, Foster 1988b), desiccation due to winter winds (Hadley and Smith 1986, Maruta and Nakano 1999), desiccation and mechanical damage due to summer winds (Kai 1974, Oka 1983, Kohyama 1988), increased root damage from the swaying of trees in the wind (Marchand et al. 1986), and accelerated death of stressed

Received 16 March 2017, Accepted 7 February 2018
1) Tama Forest Science Garden, Forestry and Forest Products Research Institute (FFPRI)
2) Faculty of Agriculture. Kagoshima University
3) Department of Plant Ecology, FFPRI
4) Forestry and Forest Products Research Institute
5) Japan International Forestry Promotion and Cooperation Center
* Tama Forest Science Garden, FFPRI, 1833-81 Todori, Hachioji, Tokyo, 193-0843 JAPAN; e-mail: kojiro@ffpri.affrc.go.jp

trees by bark beetle infection (Ohtaka et al. 2002). Within a strip of dead trees, vigorous regeneration of seedlings occurs (mostly through the release of formerly suppressed seedlings). Multiple developmental stages of community dynamics can thus be observed in wave-regenerated forests at any one point in time (Oshima et al. 1958, Tadaki et al. 1977, Sprugel 1984, Ugawa et al. 2007). Some studies have estimated changes in stand biomass and productivity with the development of wave-regeneration by establishing experimental plots within various aged stands (or different developmental stages) (Tadaki et al. 1977, Sprugel 1984).

However, the forests in these studies were assumed to be in a shifting-mosaic steady state, which is only in equilibrium when disturbances are sufficiently frequent and small in scale relative to the landscape, and where most dynamic processes are distributed evenly over the whole area (Sprugel and Bormann 1981). Many studies have suggested that the maintenance of wave-regeneration is accompanied by gradual degradations of canopy trees due to continuous stress (e.g. Oshima et al. 1958, Tadaki et al. 1977, Sprugel and Bormann 1981). Such studies have not given consideration to large-scale disturbances, which are caused by low frequency events such as severe windstorm or fire. Tropical cyclones (called "typhoons" in the western North Pacific) often affect forest structure and function in tropical to temperate regions, causing uprooting and defoliation of trees due to strong winds (Chambers et al. 2004, 2007, Lin et al. 2011). For coniferous forests in cool temperate and subalpine regions, cyclones sometimes cause serious damage, such as windthrow of large trees across vast areas (Kimura et al. 1986, Foster 1988a, Yamanaka et al. 1994, Ishizuka et al. 1997, Suzuki et al. 2013). These intensive disturbances can lead to major modification of the forest structure and dynamics.

In 1959, typhoon Vera (known as the Isewan typhoon in Japanese) impacted on an extensive area of forest in central Japan and caused severe windthrow of large sized trees (Morita 1960), including a wave-regenerated forest on Mt. Shimagare (Tanabe 1960, Okuhara 1977, Kimura 1982). In this forest, it was observed that most trees within the mature tree zones were damaged and that the dead tree zone became wider after the typhoon disturbance (Okuhara 1977, Kohyama and Fujita 1981). A few decades later, damaged stands have recovered mainly through natural regrowth, retaining the familiar wave patterns (Kohyama and Fujita 1981, Kimura 1982). More recently, however, it was found that stand structures and age composition were greatly modified from those observed before the disturbance, shifting to smaller and younger trees (Suzuki 2003) and showing greater heterogeneity in spatial distribution of trees (Suzuki et al. 2009, 2013). These patterns were considered to result from differences in the spatial distribution of advanced seedlings and saplings that were left over after dying of canopy trees by the typhoon disturbance (Suzuki et al. 2013). These structural changes and local heterogeneity may alter the carbon dynamics of wave-regenerated forest, but there is still no information on biomass dynamics following these intense disturbances. Future climate change is predicted to change the frequency and intensity of natural disturbance to forest ecosystems through events such as wind storm and fire (Dale et al. 2001, Pechony and Shindell 2010), so has the potential to reduce net carbon stocks (IPCC 2013).

In this study, we characterize biomass dynamics in a wave-regenerated fir forest following blowdown by typhoon Vera in 1959. We reconstructed the process of biomass dynamics over time and examined influencing factors, focusing on interactions between pre- and post-disturbance stand structures such as seedling density, which were playing a key role in biomass accumulation. We discuss to what extent the potential carbon stocks would differ in disturbed forest from those in non-disturbed stands by comparing published data of biomass accumulation in undisturbed wave-regeneration forests.

2. Materials and methods

2.1 Study site

This study was carried out in the subalpine conifer forest located on the southwestern slope of Mt. Shimagare (36° 4' N, 138° 20' E; 2403m a.s.l.) in the Northern Yatsugatake Mountains of central Japan (Fig. 1). Annual mean air temperature at the study site was about 1.9°C during the study period (2001-2008), estimated from the data recorded at the nearest AMeDAS station at Suwa city (about 20km southwest from the site). Annual precipitation recorded at the station averaged about 1200mm during the period. Snowfall at the site generally occurs from November to March, and snow accumulation continues from early December to late May.

The bedrock at Mt. Shimagare is andesite originating from volcanic eruptions in the mid- to late Pleistocene (Kawachi 1974). The soil is moderately moist and dark brown, falling into the FAO classification of Cambisol (Ugawa et al. 2010), and ground floor is covered with mosses, needle litters and humus. The mineral soil is relatively thin (30-40cm deep), permitting only the development of shallow tree root systems (Oshima et al. 1958). The study forest was dominated by two subalpine *Abies* species, *A. veitchii* Lindley and *A. mariesii* Mast., together with several other species, such as *Picea jezoensis* Carr. var. hondoensis (Mayr) Rehder, *Betula ermanii* Cham. and *Sorbus commixta* Hedl. (Oshima et al. 1958).

Before typhoon Vera, Yoshida and Yamanouchi (1955) established a 530m-length belt transect on the study slope. The same transect has been studied repeatedly in four different

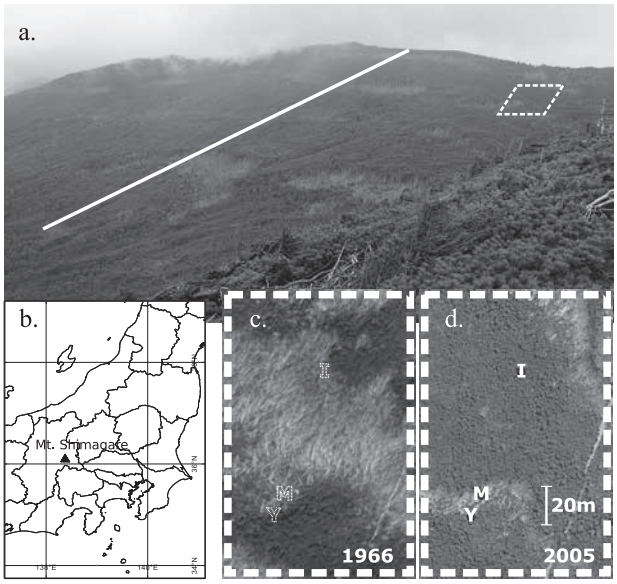

Fig. 1. Location and views of the study site.
(a) study site (dashed line square) on the southwestern slope of Mt. Shimagare, inset in (c) and (d); the solid white line shows the approximate location of the belt transect defined by Yoshida and Yamanouchi (1955). (b) Location of Mt. Shimagare on Honsyu Island, Japan. Aerial photographs around the research stands were taken in 1966 (c) and 2005 (d). Y, I and M in (c) and (d) show the locations of research stands that we settled in this study.

years (1954, 1977, 1987 and 2002) (Yoshida and Yamanouchi 1955, Okuhara 1977, Maeda and Shiratori 1987, Suzuki 2003). Using the data of mean heights in sub-quadrats along the transect published in these studies, we reconstructed a stand profile diagram (Fig. 2) to illustrate how the wave-like forest has shifted along the transect over the period of ca. 40 years following the typhoon disturbance. In 1954, prior to typhoon Vera, the mean tree height increased gradually down the slope within a single wave, then decreased abruptly at the lower edge of the wave (Fig. 2a). In 1977, 18 years after the disturbance, the mean tree height in each wave was smaller (about 10m) than that in 1954 (about 13m) (Fig. 2b). In addition, waves moved up the slope by some 70-90m, and the width of the stripe of dead trees found between waves was observed to be wider (Fig. 2a, b). These structural changes suggested that the typhoon disturbance event had accelerated tree mortality and gap movement (Kohyama and Fujita 1981, Oka 1983). Mean tree heights inside the waves were further reduced (to 7-8m in 1987 and 5m in 2002), while tree heights in the gaps became larger (Fig. 2c, d). Consequently, the forest in this study period is characterized by large irregular canopy openings caused by the typhoon (e.g., Kohyama and Fujita 1981) and by tree size and age structures that differ markedly from those of wave-regenerated forests that have not experienced a major disturbance event.

2.2 Field measurements

2.2.1 Tree census

In 2001, three research stands were selected as representatives of different developmental stages, i.e. young (Y), intermediate (I), and mature (M) stands. The median ages of *Abies* trees were 19 years in stand Y, 36 in stand I and 59 in stand M. Tree ages were estimated by counting the number of tree rings at the soil surface for each sample individual felled in 2002 (see below). Two 5m×5m plots were established in each stand for the purpose of obtaining tree census data. The plots were selected to represent high (h) and low (l) tree densities in each stand.

In each plot, we measured stem diameter at 1.3m height ($D_{1.3}$), height of crown base from the ground (H_B) and tree height (H) for all living trees taller than 1.3m of the two *Abies* species. We also recorded evidence of notable damage, such as stem breakage. For smaller trees ($0.3m \leqq H < 1.3m$), stem diameters at 0.1m height ($D_{0.1}$), stem diameters at crown base (D_B), HB and H were measured. For the two plots in stand Y, $D_{0.1}$ measurement were recorded for all trees, regardless of their heights, since many trees were below 1.3m in height and these trees were difficult to divide two layers, when we had measured first time in 2001. The tree census was conducted once a year in early June from 2001 to 2008.In June 2001 data for plot Y_1 was not collected: censuses were complete for all following years.

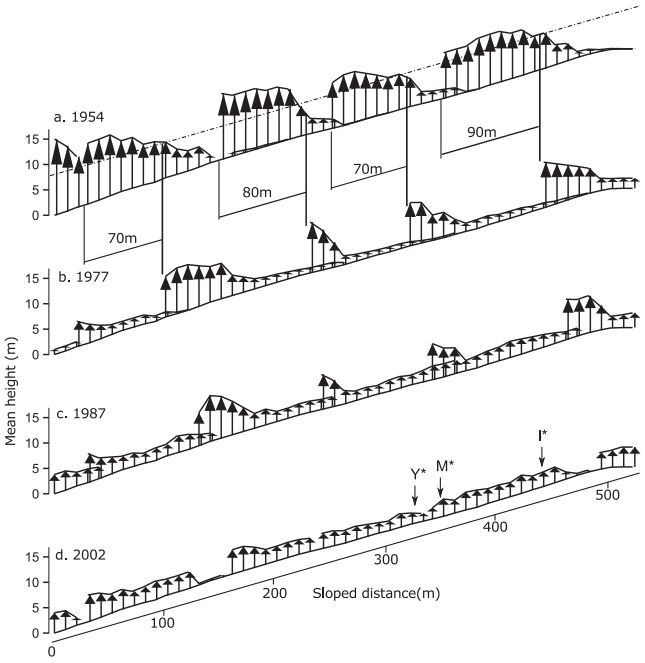

Fig. 2. Changes in mean tree heights along the slope of a wave-regenerated *Abies* dominated forest on Mt.Shimagare from 1954 (before typhoon Vera) to 2002. Data from permanent belt transect along the slope, 530m in length and 10m in width (Yoshida and Yamanouchi 1955, Okuhara 1977, Maeda and Shiratori 1987, Suzuki 2003). Redrawn from Maeda and Shiratori (1987), and data added from Suzuki (2003). Mean tree height in each 10x10m (sloped distances) sequential quadrat shown. Dashed dotted line shows 8m height, showing the boundary of height dependent typhoon disturbance on canopy trees, estimated from a comparison of the stand profiles from 1954 (a) to 1977 (b). Y*, I* and M* show the relative locations of the young, intermediate and mature stands examined in this study.

2.2.2 Tree sampling

In October 2002 and 2003, we sampled 31 trees to establish size-dry mass allometric equations (n=16 for *A. veitchii*, n=15 for *A. mariesii*; using five or six trees per species in each stand). The height ranges of the sample trees were 0.41-2.92m in stand Y, 2.94-5.95m in stand I and 2.43-7.12m in stand M. The sample trees were felled at ground surface level and four size parameters, $D_{1.3}$, H, H_B, and D_B, were measured. For the smaller sample trees in stand Y, $D_{0.1}$ was measured instead of $D_{1.3}$. Each sample tree in stands I and M was divided into 1-m vertical segments, and the fresh masses of the stem and branches with needles in each segment were measured separately. Stems of sample trees in stand Y were cut into shorter segments (0.125-0.5m in length). In each segment, several branches (with needles) were randomly sampled for determining relative proportion of needles, and stem disks were removed from the lower-most segment. Current branches (i.e. with needles) were removed from older parts of samples and weighed to quantify their fresh masses separately. These samples were taken to the laboratory and needles were removed from each branch samples. All samples (stem, current branches and needles, older branches and needles) were oven-dried at 70°C for three to seven days until weights remained constant, and the dry/fresh ratio of each component was determined. Using these data, the dry masses of stem (W_S), branches (W_B) and needles (W_N) of each sample tree were calculated.

2.3 Data analysis

To examine the growth patterns of *Abies* trees in each study stand, fluctuations in annual ring widths were analyzed for the stem disks taken at the lowermost section of the sample trees. Annual ring widths were measured in four directions in the cross section.

To estimate the individual- and stand-level biomass of the four tree components (stem, branch, needle, coarse root), we developed nonlinear model equations based on allometric relationships between observed size parameters ($D_{1.3}$ or $D_{0.1}$, H and H_B) and each component dry mass. Details of model selection and fitting method are summarized in the Appendix, and the final models selected are shown in Appendix Table 2. The coefficients of the selected models that we used were

different between the two tree species. Yearly changes in the biomass of each of the tree component within the six study plots were reconstructed using these nonlinear model equations. Here, both of the biomass of undamaged *Abies* trees and those that were affected by shoot damage were estimated using the same prediction formula. The biomass of *Betula* trees which grew only in the high-density, intermediate aged stand (I_h), was ignored due to its relatively minor overall contribution.

Patterns of yearly changes in plot biomass were compared between the two different density plots (high, low) within each stand, using a linear mixed model to test for differences in initial biomass and annual biomass increment on time course data in each plot. The following model was fitted to the data in each stand:

$$\text{Model1: } W = \beta_0 + \beta_1 DENSITY + \beta_2 YEAR + \beta_3 DENSITY{:}YEAR + R + \varepsilon$$

where the yearly change in total biomass in each plot (W) was given as the linear regression of two factors: *YEAR* (years from 2001: 0-7) and *DENSITY* (plot densities: high=0 and low=1), and their interaction *DENSITY:YEAR*. R indicates random effects of plots. In this model, the coefficients (β_0, $\beta_0+\beta_1$) describe the initial biomass, and (β_2, $\beta_2+\beta_3$) the annual increments in high and low density plots respectively.

For comparison of biomass differences among the stands, we fitted another linear model separately to each series of the high and low density plots in the Y, I and M stands.

$$\text{Model2: } W = \beta_0 + \beta_1 STANDY + \beta_2 STANDM + \beta_3 YEAR + \beta_4 STANDY{:}YEAR + \beta_5 STANDM{:}YEAR + R + \varepsilon$$

where STANDY and STANDM are dummy variables denoting stands.

The two *Abies* species were distinguished in the field measurements and during sampling, but were treated together in the data analysis.

3. Results

3.1 Stand structure change

Table 1 summarizes tree size parameters, stand structure variables and each component biomass obtained in each plot at the beginning (2002) and end of the study period (2008). In 2002, the densities of *Abies* trees (3.20-4.68m^{-2}) in the high density plots (Y_h, I_h, M_h) were approximately twice those (1.40-2.16m^{-2}) in each corresponding low density plot (Y_l, I_l, M_l). Of the high density plots, *Abies* density was highest in Y_h and similar between the I_h and M_h plots. The densities decreased in all high density plots and one low density plot (M_l) during the study period, while they remained similar in the other two plots (Y_l and I_l) (Table 1, see also Fig. 3). In stand M, which was located adjacent to a dead tree zone of wave-regeneration, some canopy-layer trees were observed to decline (i.e., crown

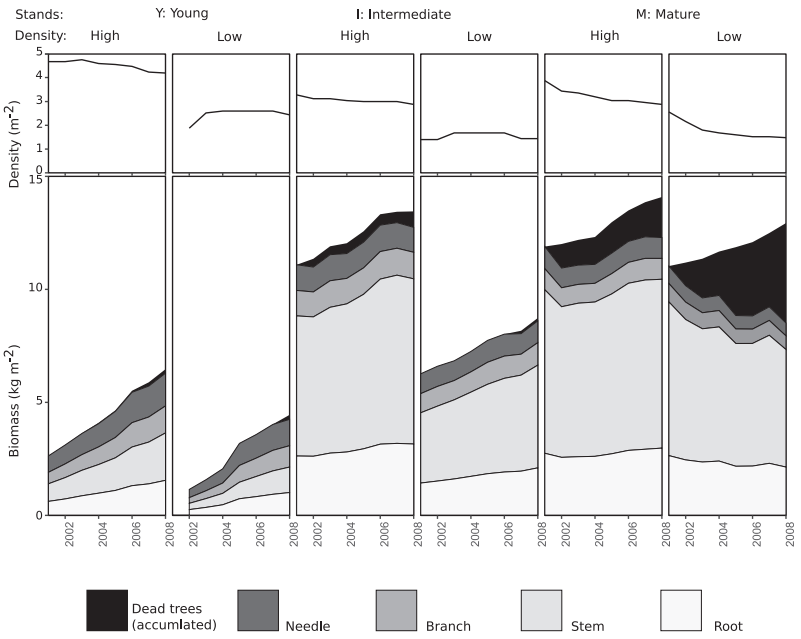

Fig. 3. Changes in the tree density and biomass of each tree component (stem, branch, needle coarse root and accumulated loss with dead trees) for six study plots in the years 2002-2008.

Table 1. Outline of the study plots.

Stand	Y				I				M			
Age (median(range))	18(15-29)				35(32-74)				58(46-66)			
Plot	Y_l		Y_h		I_l		I_h		M_l		M_h	
year	2002	2008	2002	2008	2002	2008	2002	2008	2002	2008	2002	2008
Density (m^{-2})	1.88	2.44	4.68	4.2	1.4	1.44	3.2	2.96	2.16	1.48	3.44	2.88
Mixture ratio (%)												
Abies mariesii	0.7	0.77	0.71	0.68	0.29	0.25	0.5	0.5	0.52	0.46	0.41	0.4
Abies veitchii	0.3	0.23	0.29	0.32	0.71	0.75	0.48	0.47	0.48	0.54	0.59	0.6
Betula ermanii							0.03	0.03				
Height, H (m), mean	1	1.6	1.3	1.9	2.7	2.8	3	3.3	3.8	3.8	3.1	3.4
(min-max)	0.6-1.7	0.5-3.0	0.4-2.3	0.4-3.4	0.6-5.3	0.5-6.3	0.6-5.5	0.6-6.1	0.7-6.7	0.5-7.0	0.5-6.0	0.4-6.4
Crown length, C(m)												
mean	0.9	1.2	0.9	1	1.3	1.2	1	1	1	0.9	0.8	0.9
(min-max)	0.5-1.6	0.2-2.9	0.1-2.1	0.0-3.1	0.1-3.8	0.0-4.3	0.0-3.2	0.0-3.3	0.0-3.6	0.0-3.2	0.0-2.7	0.0-3.7
C / H, mean	0.87	0.73	0.7	0.5	0.4	0.32	0.29	0.24	0.22	0.26	0.21	0.22
(min-max)	0.74-0.97	0.31-1.00	0.10-0.96	0.01-0.94	0.10-0.73	0.03-0.67	0.03-0.62	0.02-0.53	0.01-1.00	0.01-0.83	0.00-0.53	0.02-0.63
Upper layer (H>1.3m trees in I and M)												
$D_{1.3}$ (cm), mean					5.8	6.8	4.7	5.1	5.3	6.4	4.5	5.1
(min-max)					2.9-11.1	3.5-13.1	1.9-10.5	1.7-11.5	1.7-10.6	2.5-11.6	1.8-8.9	2.0-9.9
$H/D_{1.3}$, mean					68	67	82	79	90	85	84	81
(min-max)					47-86	49-79	45-143	49-143	60-124	60-111	63-116	60-111
$BA_{1.3}$ (cm^2 m^{-2})					25.4	32.8	48.9	56.4	43.4	34.7	49.4	53.9
Lower layer (0.3m< H≦1.3m trees in I and M, 0.3m< H trees in Y)												
$D_{0.1}$ (cm), mean	2.3	3.5	2.4	3.4	1.9	1.8	2.2	2.1	1.8	2.1	1.7	1.8
(min-max)	0.9-4.8	0.9-9.0	1.0-6.4	1.2-8.4	0.8-2.6	0.9-2.6	1.3-3.6	1.3-3.5	1.0-2.7	1.2-3.5	0.8-2.9	1.0-2.9
$H/D_{0.1}$, mean	46	48	58	59	56	52	50	48	65	49	58	52
(min-max)	24-70	14-83	26-115	19-143	39-72	32-75	30-72	31-76	48-85	35-69	41-77	43-73
$BA_{0.1}$ (cm^2 m^{-2})	9.1	29.1	25.3	45.7	1.7	1.7	3.1	2.3	1.4	2	2	1.6
Biomass estimated												
(kg/m^2 (%))	1.1(100)	4.2(100)	3.1(100)	6.3(100)	6.6(100)	8.6(100)	11(100)	12.7(100)	10.2(100)	8.5(100)	10.9(100)	12.3(100)
Needle	0.4(32)	1.2(27)	0.8(27)	1.4(23)	0.9(14)	1.0(11)	1.1(10)	1.1(9)	0.7(7)	0.6(7)	0.9(8)	0.9(8)
Branch	0.3(22)	0.9(22)	0.6(19)	1.2(19)	0.9(13)	1.0(12)	1.1(10)	1.2(9)	0.8(8)	0.6(7)	0.8(8)	0.9(8)
Stem	0.3(24)	1.1(27)	0.9(30)	2.1(33)	3.3(50)	4.5(53)	6.2(56)	7.3(57)	6.2(61)	5.2(61)	6.7(61)	7.5(61)
Root	0.3(22)	1.0(24)	0.7(24)	1.5(25)	1.5(23)	2.1(24)	2.6(24)	3.2(25)	2.5(24)	2.1(25)	2.6(23)	3.0(24)

Y, I and M in the stand show young, intermediate and mature stand respectively, Subscript h and l in plot name represent high- and low- density respectively, $D_{1.3}$ and $D_{0.1}$ show stem diameter at 1.3m height and at 0.1m height, $BA_{1.3}$ and $BA_{0.1}$ show basal areas at 1.3m height and at 0.1m height.

Table 2. Regression results of the selected models for annual changes of the biomass estimates in each plot

Model 1: $W = \beta_0 + \beta_1 DENSITY + \beta_2 YEAR + \beta_3 DENSITY{:}YEAR + R$

Factors: *YEAR:* years from 2001 (0-7)

DENSITY: plot densities High=0 and Low =1

R : Random effects of plots

Coefficients:

STAND	β_0	β_1	β_2	β_3	R SD	residuals SD
Young	2.53	-1.87	0.54		$1.5e^{-6}$	0.16
Intermediate	10.86	-4.56	0.32		$1.7e^{-6}$	0.18
Mature	11.11	-0.55	0.16	-0.46	$3.3e^{-6}$	0.36

Interpretation of coefficients:

β_0 and $\beta_0 + \beta_1$: initial biomass in high and low density plots

β_2 and $\beta_2 + \beta_3$: annual increments in high and low density plots

Model 2: $W = \beta_0 + \beta_1 STANDY + \beta_2 STANDM + \beta_3 YEAR + \beta_4 STANDY{:}YEAR + \beta_5 STANDM{:}YEAR + R$

Factors: *YEAR*: years from 2001 (0-7)

STANDY: The young stand=1, others=0

STANDM: The mature stand=1, others=0

Coefficients:

STAND	β_0	β_1	β_2	β_3	β_4	β_5	R SD	residuals SD
High density	11.01	-8.43		0.29	0.25	-0.11	$2.3e^{-6}$	0.27
Low density	6.27	-5.68	4.29	0.33	0.23	-0.63	$1.0e^{-6}$	0.24

Interpretation of coefficients:

β_0, $\beta_0 + \beta_1$ and $\beta_0 + \beta_2$: initial biomass in the stands I, Y and M

β_3, $\beta_3 + \beta_4$ and $\beta_3 + \beta_5$: annual increments in the stands I, Y and M

dieback) and some died within both study plots (M_l and M_h) during the study period. The mean H, which was highest in stand M and lowest in stand Y, increased in all plots during the study period. The mean crown length C = H-H_B ranged from 0.8m in M_h to 1.3m in I_l and was greater in the low density plot (Y_l, I_l, M_l) than in the corresponding high density plot (Y_h, I_h, M_h) in each stand. Mean C was shortest in M_h among the high density plots. The mean ratios of C to H were largest in stand Y and decreased in order of Y, I, M and was higher in the low density plot than in the corresponding high density plot in each stand. The mean $D_{1.3}$ in the four plots in stand I and M increased during the study period. Mean $D_{1.3}$ values in the two mature plots (M_l, M_h) were similar to those in the two intermediate-age plots (I_l, I_h). The mean ratios of H to $D_{1.3}$ in the four plots in stands I and M ranged from 67 in I_l to 90 in M_l and were smaller in stand I than in stand M. In stand I, $H/D_{1.3}$ ratios were smaller in I_l than in I_h.

3.2 Tree growth patterns

We counted 47-67 annual tree rings for the sample trees in stand M, 33-72 in stand I, and 15-30 in stand Y (Table 1). By calculating from the year when each tree was felled (2002 in the I and M stands, 2003 in the Y stand), the innermost tree rings were formed in the years 1936-1956 in stand M, 1931-1970 in stand I, and 1974-1989 in stand Y. As for stand I, a single tree had 72 rings, while the other nine trees were much younger, with a narrow range of 33-38 rings, indicating that the sample trees were mostly established at similar period (1965-1970).

Tree ring analysis showed that growth patterns of the sample trees differed among the three stands (Fig. 4). In the stand M, the sample tree diameters increased slowly in their early years (1940-50s), and the growth of some trees increased sharply from 1959 onwards. On the other hand, in the stand I, many of the sample tree diameters increased linearly from their early stages. In the stand Y, diameter growth gradually increased during the trees' initial stages of development. In yearly changes of mean width of tree rings in the stands, monopodial patterns were shown in stand I and M with their peak in 1980 and 1966 respectively (Fig. 4). The peak value of mean width was smaller in stand M than in other two stands. From these patterns, we divided them to three phases, i.e., Phase 1, where ring width fluctuations remain low, Phase 2: where ring width rapidly increase, Phase 3: where they decrease gradually with annual fluctuations. In stand Y, they increased monotonously and were not considered to have reached Phase 3 yet. For comparing the increasing rates of tree ring width in the phase 2 among the stands, a linear mixed effects model that include effects of elapsed years, the stands and their interactions with individual trees as a random effect was fitted on these data. The fixed effects of interactions between elapsed time and stand were not significant ($p > 0.05$). It showed that increasing rates of tree ring width in Phase 2 were not significantly different among stands.

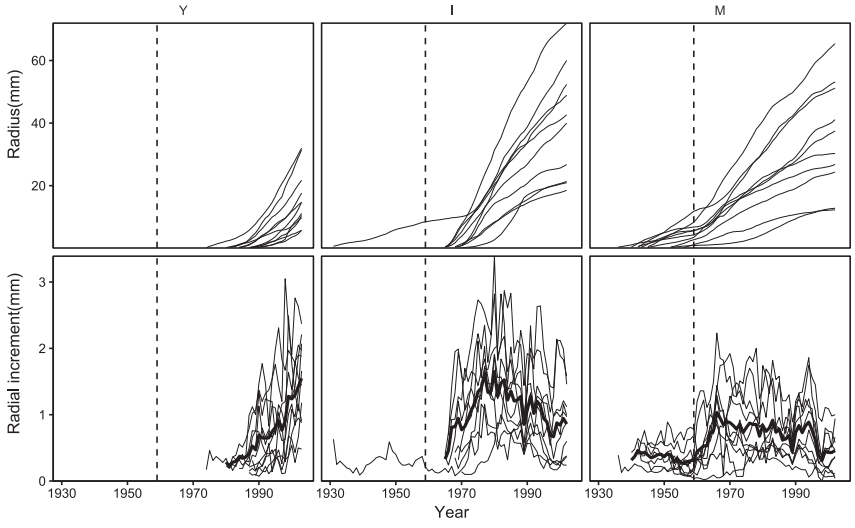

Fig. 4. Changes in radiuses and their annual increments of tree rings at soil surface level for each sample tree of young (Y), intermediate (I) and mature (M) stands.
Bold lines show annual means of radial increments in each stand. Vertical dashed line indicates the year 1959 when typhoon Vera attacked.

3.3 Biomass change

Total and each component biomass increased in all the study plots except M_l during the study period. Biomass was highest in plot I_h, and similar between plots I_h and M_h in 2001(Fig. 3). According to the model selections from subsets of Model1, the model including the major effects of *DENSITY, YEAR* and the interaction effect of *DENSITY:YEAR* was selected for fitting to the stand M data, whereas the effects of *DENSITY:YEAR* were excluded in the model selected for stands Y and I (Table 2). These results indicated that initial biomass was lower in the low density plot than high density plot in each stand, and rates of biomass increment did not differ between the high- and low-density plots in stands Y and I. Consequently, the annual biomass increment in each plot, which were estimated by the parameters of Model1, was 0.54kg m^{-2} $year^{-1}$ in stand Y, 0.32kg m^{-2} $year^{-1}$ in stand I, 0.16kg m^{-2} $year^{-1}$ in plot M_h and -0.30kg m^{-2} $year^{-1}$ in plot M_l. As mentioned above, several large canopy-layer trees of the mature stand (M) had declined and died during the study period, which greatly contributed to the continuous reduction of biomass in plot M_l during the study period (Fig. 3). In the results from the model selections from subsets of Model2, the effect *YEAR* and its interactions with stand *STANDY:YEAR, STANDM:YEAR* were selected in both sets of the different densities. Biomass increment was largest in stand Y, followed by stands I and M (Table 2).

Each estimate of needle and branches biomass increased rapidly over time in stand Y, whereas they stayed at almost constant levels in the high-density plots in stands I and M during the years 2001 to 2008 (Table 1, Fig. 3). On the other hand, the relative proportion of biomass in stems increased in stands Y and I, with a corresponding decrease in that of needles (Table 1, Fig. 3). When the two plots of different densities were compared for each stand, the estimates of biomass in branches and needles were smaller but their relative proportions were greater in the low-density plot than the high-density plot.

4. Discussion

We compared the temporal trends in aboveground biomass in our study site with the results from three previous studies conducted in wave-regeneration forests (Fig. 5). One site was located in the vicinity of our site, Mt. Shimagare, from which biomass data were obtained before the Typhoon Vera event (Oshima et al. 1958). Other sites were located on Mt. Asahi (about 36km from our study site), where the typhoon disturbance was not serious (Tadaki et al. 1977), and on Whiteface mountain, North America (Sprugel 1984). These previous studies share a similar pattern, increasing rapidly in young stands (30-40 years), then increasing monotonously until 60-100 years of age (Fig. 5). Our study results also followed those patterns. However, the biomass estimates in stand M (about 8-9kg m^{-2}; M_h, M_l) were smaller than those of the similar-aged (> 60 years) stands in the previous studies. There were comparable amounts with that in stand I, which was about 20 years younger than stand M. We observed the death of several canopy trees in stand M during the research period and many trees had already exhibited symptoms of dieback. Though previous studies noted that mortality of overstory trees in wave-regeneration forests occurs at 80 - 100 years (Oshima et al. 1958, Kohyama and Fujita 1981), the onset of mortality started earlier in stand M, at ca. 60 years old. This reduction of age and tree sizes in mature stands could be related to the typhoon disturbances that had accelerated tree mortality and increased gap movement, as already described in the section 2.1. We could not estimate overall variations in tree sizes on whole areas of the forest from using these results from the limited sample areas. However, recent studies on Mt. Shimagare showed that tree size compositions in mature tree stands were similar to those that we observed (Suzuki 2003 (Fig. 2d), Ugawa et al. 2007). It suggests that the reduction in biomass that we found prevail on the slopes of Mt. Shimagare.

To examine the linkage between the observed patterns in biomass and stand structural change, we superimposed the relative position of each study stand on the diagrams of stand profile (see marks Y*, I*, M* in Fig. 2d) of a nearby transect along wave-regeneration forest (Fig. 1) where past stand structure has been reconstructed repeatedly since 1954 (see Methods). According to the virtual plot location, the current young stand (Y*) is considered as a formerly intermediate-aged stand when typhoon Vera struck in 1959 (see diagram in 1954; Fig. 2a). Likewise, the intermediate (I*) and mature (M*) stands correspond to formerly mature and young (or overmature) stands, respectively. Comparison of the stand profiles from 1954 to 1977 (Fig. 2a, b) indicates that the typhoon windthrow occurred in stands where the mean height of canopy trees exceeded approximately 8 m. Fig. 1c shows that there were still many windthrown trees on the forest floor, and that only the stand I* was located within a large windthrown area when the aerial photograph taken in 1966, eight years after the typhoon. This evidence suggests that only the stand I* sustained destructive typhoon damage on canopy-layer trees, whereas the other two sites, M* and Y*, escaped serious damage because there were few or no canopy-layer trees (H >8m) present at that time.

The difference in the magnitude of disturbance by growth stage may also have affected post-disturbance regeneration processes and growth conditions of seedlings. Positive growth response of seedlings often appears due to improved light conditions following windthrow events (Kimura et al. 1986).

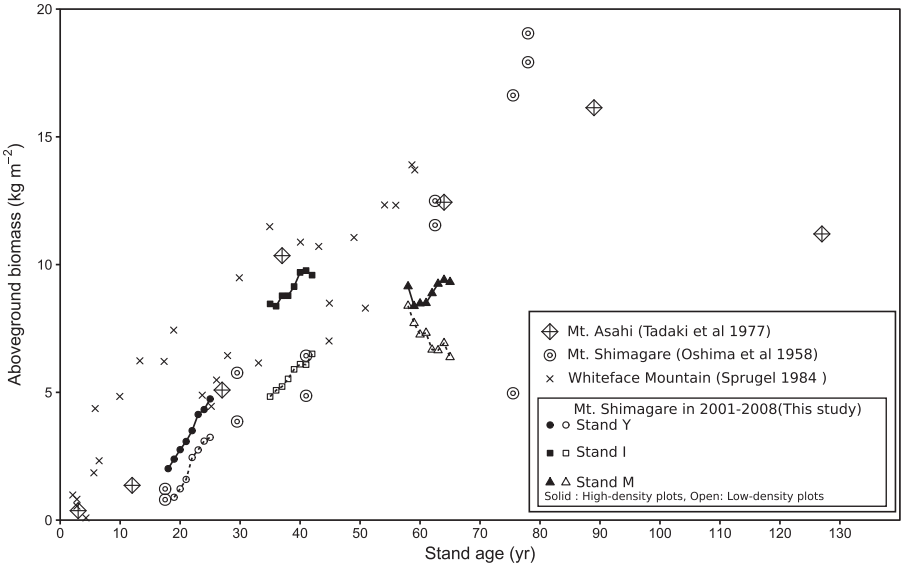

Fig. 5. Relationships between aboveground biomass and stand age of six study plots in wave-regeneration forests on Mt. Shimagare from 2001-2008.
Stand Y: young stand, Stand I: intermedate stand, Stand M: mature stand. Data from three previous studies are also indicated: one in wave-regeneration *Abies* forests on Mt. Asahi (Tadaki et al. 1977), another in pre-disturbance, wave-regeneration fir forests on Mt. Shimagare before typhoon Vera (Oshima et al. 1958) and the other in Whiteface Mountain, USA (Sprugel 1984). For the data of Oshima et al. (1958), the aboveground biomass in each plot was calculated by multiplying aboveground total dry mass of standard-size sample trees and tree density. Note that each stand age was estimated by the number of stem rings at 50cm height in Sprugel (1984), at soil surface in other studies.

The recovery of a subalpine coniferous forests following a windthrow event was dependent on both the release of previously suppressed, advanced seedlings and newly recruited seedlings (Kohyama 1984, Kimura et al. 1986, Yamamoto 1996, Kulakowski and Veblen 2003). The state of the seedling bank varies depending on the condition of the canopy trees and the light conditions (Kohyama 1984). In mature wave-regenerated forests close to dieback zones, seedling populations become established in high densities following gradual changes in light conditions on the forest floor (Kimura 1982). For example, Ugawa et al. (2010) suggested that *Abies* seedlings can establish in mature stands with fewer than 6,000 trees per hectare (>6% relative light intensity). It was shown that seedlings were established approximately 30-70 /m^2 at young stands in 1958 (Oshima et al. 1958). As mentioned above, the stand M was considered to be a similar young stand at that time (Fig. 2), so it was speculated that the forest in stand M had been grown from such a high densities of seedling community, with large mortalities due to self-thinning. On the other hand, the faster growth of trees in stand I than in stand M (Fig. 4) may result from more favorable light conditions for post-typhoon seedlings. These are found under the condition of lower seedling densities under the larger canopy openings. In the results from tree-ring analysis, all of the sample trees in site M showed symptoms of suppression, but in site I most sample trees grow rapidly from their initial phase (Fig. 4). Therefore, biomass accumulation largely depended on seedlings that germinated after the typhoon disturbance in stand I, whereas in stand M biomass accumulation relied on more advanced seedlings already recruited there (i.e., pre-typhoon seedlings). In addition, maximum value of mean annual increments was smaller in stand M than in other two stands. This result also supported that the forest in stand M had been grown from higher densities of seedling community than in other stands, considering that tree radial growth were majorly regulated by competition among neighboring trees (Kunstler et al. 2011). These results suggested that stand I growth could achieve a rate of biomass accumulation as high as that of stand M in a shorter period, mainly due to faster individual growth rates. The positive growth response which can be expected after a severe disturbance thus happens only under a particular combination of stand structure and seedling type. To evaluate more large-scale variations in seedling growth response and its contribution to stand-level biomass

accumulation, we must examine other relevant growth factors or inhibitors of seedling establishment processes, such as heterogeneity in seed dispersal, accumulation of windthrown tree boles and competition with tall herbs (Rammig et al. 2006, 2007). Suzuki et al. (2013) examined stand structures in wave-regeneration fir forest close to our study site, showing that a large degree of heterogeneity in tree distribution still existed 45 years after Typhoon Vera, and suggested that differences in the density and spatial distribution of seedlings produced at the time of disturbance persisted and gave rise to the heterogeneity.

The biomass of branches and needles increased rapidly in stand Y, whereas they had near-constant values in stands I and M (Table 2, Fig. 3). The biomass of stems and coarse roots increased perceptibly in all stands. Consequently, the relative biomass proportion of stems and roots increased in all stands during the study period (Fig. 3).The pattern of biomass allocation is similar to those reported in other wave-regeneration subalpine forest studies without wind storm disturbance (Tadaki et al. 1977, Sprugel 1984). The foliage biomass in our study forest, ranging from 0.92-1.17kg m^{-2} (maximum 1.45kg m^{-2} in the young stand Y_h) (Table 2), is nearly equivalent to the estimated range (0.86-1.05kg m^{-2}) and maximum (1.21kg m^{-2}) in a young stand (13 yrs-old) in the wave-regeneration forest on Mt. Shimagare before the Typhoon Vera damage (Oshima et al. 1958).This suggests that the foliage biomass of the typhoon-disturbed forest has already recovered to the same level as before the typhoon, although the total stand biomass has not yet fully recovered (Fig. 5).

5. Conclusion

In this study, we showed that heterogeneity of seedling distributions that were caused by typhoon disturbance affect subsequent forest structures and biomass accumulation. On the other hand, previous studies have shown that the effects of past typhoon disturbance on the forest were confined to the reduction in size of mature trees at the forest edges and in the heterogeneity of spatial tree distributions. From these observations we speculated that biomass on the slopes of Mt. Shimagare had not yet recovered to pre-disturbance levels. As global-scale climate change is likely to influence hurricane formation (Royer et al. 1998, Dale et al. 2001), shifting storm tracks and an increasing probability of stronger typhoons making landfall are predicted around Japan (Murakami et al. 2010, Yasuda et al. 2010). To evaluate precisely the total future changes in overall carbon stocks in this forest ecosystem under any given climate change scenario, further analyses on the interaction between forest structure and biomass changes are necessary, with a particular focus on large-scale spatial heterogeneity (i.e., landscape level) effects.

Acknowledgement

We would like to thank the Nagano Prefectural Government and Japanese Forestry Agency for permission to conduct surveys in Yatsugatake-chubu Sangaku Quasi-National Park. We would also like to thank Fukuda Kenji and Suzuki Kazuo, professor of the university of Tokyo, for helpful advices from the beginnings of the research, Tabuchi Ryuichi, Hasegawa Motohiro and other researchers of FFPRI for the field survey and useful suggestions, Tate Kazuko and Michiru Ohnaka for their help in laboratory work. This research is partially supported by a grant from the Japanese Ministry of the Environment for Global Environment Research.

References

Boyce, R. L. (1988) Wind direction and fir wave motion. Can. J. Forest Res. 18, 461-466.

Chambers, J., Higuchi, N., Teixeira, L., dos Santos, J., Laurance, S. and Trumbore, S. (2004) Response of tree biomass and wood litter to disturbance in a Central Amazon forest. Oecologia, 141, 596-611.

Chambers, J. Q., Fisher, J. I., Zeng, H., Chapman, E. L., Baker, D. B. and Hurtt, G. C. (2007) Hurricane Katrina's carbon footprint on US Gulf Coast forests. Science, 318, 1107-1107.

Dale, V. H., Joyce, L. A., McNulty, S., Neilson, R. P., Ayres, M. P., Flannigan, M. D., Hanson, P. J., Irland, L. C., Lugo, A. E. and Peterson, C. J. (2001) Climate change and forest disturbances: climate change can affect forests by altering the frequency, intensity, duration, and timing of fire, drought, introduced species, insect and pathogen outbreaks, hurricanes, windstorms, ice storms, or landslides. BioScience, 51, 723-734.

Foster, D. R. (1988a) Species and stand response to catastrophic wind in central New England, USA. J. Ecol., 76, 135-151.

Foster, J. R. (1988b) The Potential Role of Rime Ice Defoliation in Tree Mortality of Wave- Regenerated Balsam Fir Forests. J. Ecol., 76, 172-180.

Hadley, J. L. and Smith, W. K. (1986) Wind Effects on Needles of Timberline Conifers: Seasonal Influence on Mortality. Ecology, 67, 12-19.

IPCC (2013) "*Climate Change 2013: The Physical Science Basis. Contribution of Working Group I to the Fifth Assessment Report of the Intergovernmental Panel on Climate Change*" . Cambridge University Press, Cambridge, United Kingdom and New York, NY, USA.

Ishizuka, M., Toyooka, H., Osawa, A., Kushima, H., Kanazawa, Y. and Sato, A. (1997) Secondary succession following catastrophic windthrow in a boreal forest in Hokkaido, Japan. J. Sustain.Forest., 6, 367-388.

Iwaki., H. and Totsuka, T. (1959) Ecological and physiological

studies on the vegetation of Mt. Shimagare II. On the Crescent-shaped "Dead Trees Strips" in the Yatsugatake and the Chichibu Mountains. Bot. Mag. Tokyo, 72, 255-260.

Kai, K. (1974) Some aspects on the Shimagare phenomenon in the subalpine forests in the Kanto and the Chubu districts, Japan. Geogr. Rev. Japan, 47, 709-719.

Kawachi, S. (1974) Geology of the Tateshinayama district. Geological Survey of Japan, Tokyo.

Kimura, M. (1982) Changes in population structure, productivity and dry matter allocation with the progress of wave regeneration of *Abies* stands in Japanese subalpine regions. In Waring, R. W. (ed.) "*Carbon Uptake and Allocation in Subalpine Ecosystems as a Key to Management*" , Proceedings of an I.U.F.R.O. workshop P. I. 07-00 Ecology of Subalpine zones. Oregon State Univ., 57-63.

Kimura, M., Kimura, W., Honma, S., Hasuno, T., Sasaki, T. (1986) Analysis of development of a subalpine *Abies* stand based on the growth processes of individual trees. Ecol. Res., 1, 229-248.

Kohyama, T. (1984) Regeneration and coexistence of two *Abies* species dominating subalpine forests in central Japan. Oecologia, 62, 156-161.

Kohyama, T. (1988) Etiology of "Shimagare" Dieback and Regeneration in Subalpine *Abies* Forests of Japan. GeoJournal, 17, 201-208.

Kohyama, T. and Fujita, N. (1981) Studies on the *Abies* population of Mt. Shimagare. Bot. Mag. Tokyo, 94, 55-68.

Kulakowski, D. and Veblen, T. T. (2003) Subalpine forest development following a blowdown in the Mount Zirkel Wilderness, Colorado. J. Veg. Sci., 14, 653-660.

Kunstler, G., Albert, C. H., Courbaud, B., Lavergne, S., Thuiller, W., Vieilledent, G., Zimmermann, N. E. and Coomes, D. A. (2011) Effects of competition on tree radial-growth vary in importance but not in intensity along climatic gradients. J. Ecol. 99, 300-312.

Lin, T. -C., Hamburg, S. P., Lin, K. -C., Wang, L. -J., Chang, C. -T., Hsia, Y. -J., Vadeboncoeur, M. A., McMullen, C. M. M. and Liu, C. -P. (2011) Typhoon disturbance and forest dynamics: lessons from a Northwest Pacific subtropical forest. Ecosystems, 14, 127-143.

Maeda, S.and Shiratori, S. (1987) Follow-up survey on Shimagare phenomena, an interim report 2. Gyomu Kenkyu Happyou Shu, Nagano Central Forest Office, 62, 17-25.

Marchand, P. J., Goulet, F. L. and Harrington, T. C. (1986) Death by attrition: a hypothesis for wave mortality of subalpine *Abies balsamea*. Can. J..Forest Res., 16, 591-596.

Maruta, E. and Nakano, T. (1999) The effects of environmental stresses on conifers in the subalpine area of the Central Japan. Jpn J. Ecol. 49(3), 293-300.

Morita, S. (1960) Showa-34-nen Taihuu Higai Hakusyo: Rinsan. Ringyo Gijutu, 220, 21-26.

Murakami, H., Wang, B. and Kitoh, A. (2010) Future change of western north pacific typhoons: Projections by a 20-km-Mesh Global Atmospheric Model. J. Climate, 24, 1154-1169.

Ohtaka, N., Masuya, H., Kaneko, S., Yamaoka, Y. and Ohsawa, M. (2002) Ophiostomatoid fungi associated with bark beetles on *Abies veitchii* in wave-regenerated forests. J. For. Res. 7, 145-151.

Oka, S. (1983) Reconsideration on the distribution of the Shimagare phenomenon in Japan. J. Geogr. 92, 1-16.

Okubo, K. (1933) On Mt. Shimagare. Jpn J. Forest., 15, 652-668.

Okuhara, T. (1977) Follow-up survey on Shimagare phenomena, an interim report. Gijutsu Kaihatsu Kenkyu-kai Syu-roku, Nagano Central Forest Office, 52, 29-37.

Oshima, Y., Kimura, M., Iwaki, H. and Kuroiwa, S. (1958) Ecological and Physiological Studies on the Vegetation of Mt. Shimagare I. Preliminary Survey of the Vegetation of Mt. Shimagare. Bot. Mag. Tokyo, 71, 289-301.

Pechony, O. and Shindell, D. T. (2010) Driving forces of global wildfires over the past millennium and the forthcoming century. Proc. Nat. A Sci. USA, 107, 19167-19170.

Pinheiro, J.C. and Bates, D.M. (2000) Mixed-effects models in S and S-PLUS. Springer Verlag New York, LLC, New York, NY, USA.

Pinheiro, J., Bates, D., DebRoy, S., Sarkar, D. and R Core Team (2015) nlme: Linear and Nonlinear Mixed Effects Models. R package version 3.1-122, URL: http://CRAN.R-project.org/package=nlme.

R Core Team (2015) R: A language and environment for statistical computing. R Foundation for Statistical Computing, Vienna, Austria. URL https://www.R-project.org/.

Rammig, A., Fahse, L., Bebi, P. and Bugmann, H. (2007) Wind disturbance in mountain forests: Simulating the impact of management strategies, seed supply, and ungulate browsing on forest succession. Forest Ecol. Manag., 242, 142-154.

Rammig, A., Fahse, L., Bugmann, H. and Bebi, P. (2006) Forest regeneration after disturbance: A modelling study for the Swiss Alps. Forest Ecol. Manag., 222, 123-136.

Royer, J. F., Chauvin, F., Timbal, B., Araspin, P. and Grimal, D. (1998) A Gcm Study of the Impact of Greenhouse Gas Increase on the Frequency of Occurrence of Tropical Cyclones. Climatic Change, 38, 307-343.

Sprugel, D. G. (1976) Dynamic structure of wave-regenerated *Abies balsamea* forests in the north-eastern United States. J. Ecol., 64, 889-911.

Sprugel, D. G. (1984) Density, biomass, productivity, and

nutrient-cycling changes during stand development in wave-regenerated balsam fir forests. Ecol. Monogr., 54, 165-186.

Sprugel, D. G. and Bormann, F. H. (1981) Natural disturbance and the steady state in high-altitude balsam fir forests. Science 211, 390-393.

Sugiura, N. (1978) Further analysts of the data by akaike' s information criterion and the finite corrections. Commun. Stat.– Theor. M., 7, 13-26.

Suzuki, K. (2003) Follow-up survey on Shimagare phenomena, an interim report 3. Nagano Ringyo Gijutsu Kouryu Happyou Shu, CHUBU Regional Forest Office, 14, 1-4.

Suzuki, S. N., Kachi, N. and Suzuki, J. -I. (2009) Changes in variance components of forest structure along a chronosequence in a wave-regenerated forest. Ecol. Res., 24, 1371-1379.

Suzuki, S. N., Kachi, N. and Suzuki, J. -I. (2013) Spatial variation of local stand structure in an *Abies* forest, 45 years after a large disturbance by the Isewan typhoon. J. For. Res., 18, 139-148.

Tadaki, Y., Sato, A., Sakurai, S., Takeuchi, I. and Teruhiko, K. (1977) Studies on the production structure of forest XVIII.: Structure and primary production in subalpine "Dead Tree Stripes" *Abies* forest near Mt. Asahi. Jpn J. Ecol., 27, 83-90.

Tanabe, K. (1960) Plants of Japan in their environment vol.1 Horizontal & vertical distribution. Hoikusya, Osaka, Japan.

Ugawa, S., Hashimoto, T., Iwamoto, K., Kaneko, S. and Fukuda, K. (2010) Relationship between stand development and establishment of seedlings in subalpine *Abies* forest. Jpn J. Forest Environ., 52, 79-86.

Ugawa, S., Iwamoto, K. and Fukuda, K. (2007) Coexistence of *Abies mariesii* and *Abies veitchii* in a subalpine fir-wave forest. Can.J. Forest Res., 37, 2142-2152.

Valentine, H. T. and Gregoire, T. G. (2001) A switching model of bole taper. Can. J. Forest Res., 31, 1400-1409.

Yamamoto, S. (1996) Gap Regeneration of Major Tree Species in Different Forest Types of Japan. Vegetatio 127, 203-213.

Yamanaka, N., Ando, M. and Tamai, S. (1994) Age structure and regeneration process of a subalpine coniferous forest in the south Japanese Alps, Central Japan. Jpn J. Forest Environ., 36, 28-35.

Yasuda, T., Mase, H. and Mori, N. (2010) Projection of future typhoons landing on Japan based on a stochastic typhoon model utilizing AGCM projections. Hydrological Research Letters, 4, 65-69.

Yoshida, K. and Yamanouchi, S. (1955) The present state of Mt. Shimagare. Zourin Gijutsu Kenkyu, Nagano central forest office, 5, 53-65.

Appendix

We used allometric equations for biomass modeling relating the component of biomass (*w*) to two predictors, tree diameter (*d*) and height (*h*)

$$w = kd^a h^b$$

An extended nonlinear model (Pinheiro and Bates 2000), based on the allometric relationship between the biomass of each component and other measured tree variables (stem diameter and stem length) with group-specific parameters (tree species and/or stands) was developed as follows.

for i=1,2,3, j=1,2, k=1,..,6

$$W_{ijk} = \exp(\varphi_{1ij}) D_{ijk}{}^{\varphi_{2ij}} H_{ijk}{}^{\varphi_{3ij}} + \epsilon_{ijk}$$

$$\Phi_{ij} = \begin{bmatrix}\varphi_{1ij}\\ \varphi_{2ij}\\ \varphi_{3ij}\end{bmatrix} = \begin{bmatrix}\beta_{11} & \beta_{12} & \beta_{13} & \beta_{14} & \beta_{15} & \beta_{16}\\ \beta_{21} & \beta_{22} & \beta_{23} & \beta_{24} & \beta_{25} & \beta_{26}\\ \beta_{31} & \beta_{32} & \beta_{33} & \beta_{34} & \beta_{35} & \beta_{36}\end{bmatrix} \begin{bmatrix}1\\ SP_j\\ STANDM_i\\ STANDY_i\\ SP_j{:}\,STANDM_i\\ SP_j{:}\,STANDY_i\end{bmatrix}$$

$$SP_j = \begin{cases}0, A.\,mariesii\\ 1,\ A.\,veitchii\end{cases}$$

$$STANDY_i = \begin{cases}1, standY\\ 0,\ standI\\ 0, standM\end{cases}$$

$$STANDM_i = \begin{cases}0, standY\\ 0,\ standI\\ 1, standM\end{cases}$$

$$\mathrm{Var}(\epsilon_{ijk}) = \sigma^2 |(fittedvalues)|^2$$

where W is an objective variable for the biomass of each component, D and H are explanatory variables denoting stem diameter and stem length (height) respectively. Parameter matrix Φ was assumed to follow a linear model that contains the factor variables of species (*SP*) and stand (*STANDY, STANDM*). Coefficient matrices are shown as β. In our preliminary examination, the within group errors in many of the fitting results showed heteroscedasticity, with a positive relationship to the fitted values. Therefore, we used the fitted values as the variance covariate. Prior to fitting the nonlinear model, we also fitted linear models that were transformed from the nonlinear model by taking the logarithm of both sides. For fitting the nonlinear model, we used the coefficients of the results of fitting the linear model as the initial values. For fitting the extended nonlinear regression model using maximum likelihood, we used R (R Core Team 2015) with the

function gnls in the nlme library (Pinheiro et al. 2015).

We used diameter at specific height D_S ($D_{1.3}$ of the trees in stands M and I and $D_{0.1}$ in stand Y) or diameter at crown base D_B as the explanatory variable of diameter D, and stem length (heights) H or Crown length $C = H\text{-}H_B$ as the explanatory variable of height H. Since the size distribution of trees differed among the study stands and measures of the height of D_S in sample trees also differed among stands, we could not separate the effects of measuring height in D_S in these models from the effect of stand Y. We regard the effect of stand Y as of the difference in measuring heights, not considering topographic and environmental differences between stands. For root biomass, we used diameter at stem base $D_{0.1}$ and $D_{1.3}$ as an explanatory variable and excluded group parameters of species and stands, because of the small sample size. When the model with $D_{1.3}$ was fit to W_R, we excluded variance covariates of fitted values, because heteroscedastic errors were not detected. For fittings to W_B and W_N, we also attempted to fit other variables in D, which is the estimated values of D_B (eD_B) from measured variables D_S, H and H_B. Equations for D_B was derived from fitting the segment model of bole taper (Valentine and Gregoire 2001) to the tree sample data. D_B were described here using this model:

$$D_B = D_S\,(C / (H\text{-}HS))^{\alpha}$$

where α was assumed to follow a linear model that contains the effect of the group variables of species and stands. Comparing the results of the fitted models with different combinations of group effects, the minimum c-AICs was in those models that have different coefficients of α between the trees in stand Y and in other stands, as follows:

$$\alpha = \begin{cases} 0.40 \in \text{stand I and M}(H > 1.3\,m) \\ 0.31 \in \text{stand Y}(H \leq 1.3m) \end{cases}$$

For model selection, we mainly used the finite collections of AIC (c-AIC, Sugiura 1978). Table A1 shows the fitting results of models, which was selected from all fitted models with different combinations of parameters of species and sites

Table A1. Fitted models

Objective variable	Explanatory variable	Parameters	Data	df	logLik	c-AIC	RSE	R^2
W_S	D_S	*STANDY*	31	5	-213.8	440	0.19	0.96
W_S	$D_S + H$	*SP + STANDY*	31	10	-189.7	410.3	0.1	0.99
W_S	$D_S + C$	*STANDY*	31	7	-204.1	427.1	0.15	0.96
W_B	D_S	*SP + STANDY + SP:STANDY*	31	9	-191.9	410.4	0.28	0.94
W_B	$D_S + C$	*STANDY*	31	7	-192.3	403.4	0.37	0.91
W_B	$D_S + H$	*SP + STANDY*	31	10	-186.2	403.5	0.33	0.95
W_B	D_B		31	3	-193.7	394.3	0.37	0.9
W_B	$D_B + C$		31	4	-190.3	390.2	0.34	0.94
W_B	$D_B + H$	*SP*	31	7	-183.4	385.8	0.29	0.9
W_B	eD_B		31	3	-193.1	393.2	0.37	0.92
W_B	$eD_B + C$		31	4	-192.2	394	0.36	0.94
W_B	$eD_B + H$	*SP*	31	7	-182.7	384.4	0.28	0.92
W_N	D_S	*SP + STANDY + STANDM*	31	9	-192.6	411.8	0.24	0.97
W_N	$D_S + C$	*SP + STANDY*	31	10	-189	409	0.31	0.91
W_N	$D_S + H$	*SP + STANDY*	31	10	-186.7	404.4	0.31	0.96
W_N	D_B	*SP*	31	5	-182.8	378.1	0.23	0.95
W_N	$D_B + C$	*SP*	31	7	-180.2	379.3	0.22	0.96
W_N	$D_B + H$	*SP*	31	8	-176.9	376.3	0.11	0.96
W_N	eD_B	*SP*	31	5	-185.1	382.6	0.25	0.96
W_N	$eD_B + C$	*SP*	31	7	-181.9	382.7	0.23	0.96
W_N	$eD_B + H$	*SP*	31	8	-177.3	377.2	0.24	0.97
W_R	$D_{0.1}$		8	3	-42.8	97.6	0.04	0.93
W_R	$D_{1.3}$		6	3	-42.9	97.9	380.4	0.95

Results showing minimum c-AIC within all fitted models with different combinations of parameters for each combination of explanatory variables tested. W_S, W_B, W_N and W_R represent the mass of stem, branch, foliage and root respectively, $D_{1.3}$ and $D_{0.1}$: stem diameter at 1.3m and 0.1m heights, D_S: diameter at specific height, $D_{0.1}$ in the stand Y samples, $D_{1.3}$ in others, D_B: stem diameter at crown base, eD_B: estimated values of D_B, H: tree height, C: length of crown, R^2: explained variation, *STANDY*, *STANDM*: dummy stand variables, *SP*: dummy species variables (Abies mariesii and A. veitchii). See Appendix for details.

for every models with different combinations of variables D and H. In the regression on stem mass W_S, the minimum c-AIC are shown in the model with D and H as variables and with group effects *SP* and *STANDY* (c-AIC=410.3, RSE=0.10, R^2=0.99). In the regressions on both branch mass W_B and needle mass W_N, the minimum c-AICs were detected in the model with D_B and H as variables and with group effects *SP* (W_B: c-AIC=385.8, RSE=0.29, R^2=0.90, W_N: c-AIC=376.3, RSE=0.11, R^2=0.96). Similar results were found between the models using eD_B and D_B. The minimum c-AIC was detected in the model with eD_B and H as variables and with group effects of *SP* (W_B: c-AIC=384.4, RSE=0.28, R^2=0.92, W_N: c-AIC=377.2, RSE=0.24, R^2=0.97). In the regression on root mass W_R, the minimum c-AIC was detected in the model with $D_{0.1}$ as a variable (c-AIC=97.6, RSE=0.04, R^2=0.93).

The final models that we used as biomass estimators are shown in Table A2. The coefficients of the selected models that we used were different between the two tree species. Yearly changes in the biomass of each sample component within the six study plots were reconstructed using these nonlinear model equations. The biomass of undamaged *Abies* trees and those that were affected by shoot damage were estimated using the same prediction formula. The biomass of *Betula* trees which grew only in the high-density, intermediate aged stand (I_h), was ignored due to its relatively minor overall contribution.

Table A2. The Equations used for biomass estimation.

Equation: $W = e^{\theta_1} D^{\theta_2} H^{\theta_3}$

Predictors: $D_{1.3}$, $D_{0.1}$: diameters at specific heights, 1.3m or 0.1m

H: tree heights

H_B: heights to the crown base

C: length of crown, H-H_B

eD_B: estimation of diameter at crown base from $D_{1.3}$, $D_{0.1}$, C

$D_{1.3}\,(C/(H\text{-}1.3))^{0.40}$ H>1.3m

$D_{0.1}(C/(H\text{-}0.1))^{0.31}$ 0.3m<H≦1.3m

Parameters:

Objective	group		D	H	$\theta 1$	$\theta 2$	$\theta 3$
Stem W_S	H>1.3m	*A. mariesii*	$D_{1.3}$	H	4.10	1.85	0.59
		A. veitchii	$D_{1.3}$	H	4.04	1.93	0.46
	H≦1.3m	*A. mariesii*	$D_{0.1}$	H	3.77	1.23	1.22
		A. veitchii	$D_{0.1}$	H	3.71	1.31	1.09
Branch W_B		*A. mariesii*	eD_B	H	2.71	2.74	-0.36
		A. veitchii	eD_B	H	2.45	2.15	0.42
Needle W_N		*A. mariesii*	eD_B	H	3.24	2.56	-0.41
		A. veitchii	eD_B	H	3.01	2.11	0.03
Root W_R	H>1.3m		$D_{1.3}$	-	2.77	2.53	
	H≦1.3m		$D_{0.1}$	-	2.66	2.40	

台風攪乱から 43 年が経過した縞枯れ林における地上部及び地下部現存量の変化

岩本 宏二郎 [1)*]、鵜川 信 [2)]、荒木 眞岳 [3)]、壁谷 大介 [3)]、石塚 森吉 [4),5)]、梶本 卓也 [3)]

要旨

大規模攪乱後の森林の再生過程を理解することは、気候変動による将来の攪乱規模の増大に対する森林の状態変化の予測に貢献する。本研究では、台風による大規模攪乱を受けた亜高山帯縞枯れ林におけるバイオマスの動態を推定することを目的として調査を行った。1959 年に伊勢湾台風によって大きな被害を受けた北八ヶ岳縞枯山において、森林の発達段階が異なる 3 林分（若齢林、中間、成熟林、それぞれ 19、36、59 年）に調査区を設置した。各調査区において、2001 年から 2008 年に繰り返し測定された毎木調査データと、サンプル木のデータにより、バイオマスが推定された。さらに、年輪解析により成長パターンを検討した。推定されたバイオマスは、若木林区で最も低かったが、中間区と成熟林区の両方で同様のレベルに達した。中間区では、風倒後に成長を開始した実生の成長が早く、前生稚樹に由来する成熟林区と同様のバイオマスになったと考えられた。大規模な攪乱がなかったと考えられる他の縞枯れ林と比較すると、特に成熟林においてバイオマスが減少していた。本調査地においては、攪乱に起因する林分構造や成熟林衰退の若齢化・サイズ減少によって台風攪乱後のバイオマスの回復は遅れているものと考えられた。

キーワード：バイオマス動態、亜高山帯針葉樹林、縞枯れ、台風攪乱

原稿受付：平成 29 年 3 月 16 日 原稿受理：平成 30 年 2 月 7 日

1) 森林総合研究所 多摩森林科学園
2) 鹿児島大学農学部
3) 森林総合研究所 植物生態研究領域
4) 元森林総合研究所
5) 国際緑化推進センター
* 森林総合研究所 多摩森林科学園　〒 193-0843 東京都八王子市廿里町 1833-81